

# Numerical Relativity

## Homework 1

Zeduri Pietro

A.Y. 2023-2024

## 1 Advection Equation:

In this first part of the homework, we will apply different numerical schemes to solve the 1D advection equation:  $\frac{\partial u}{\partial t} + \frac{\partial u}{\partial x} = 0$ , with initial condition given by the Gaussian  $u(x, t = 0) = \exp(-(x - x_0)^2)$ , where  $x_0 = 5$ ,  $x$  is limited to the interval  $[0, 10]$  and we set a terminate time to  $t = 20$ . Moreover, we will apply periodic boundary conditions, meaning that what exits the grid on one side re-enters on the opposite side. The methods we will use are the FTCS scheme (1.1), the Lax-Friedrichs scheme (1.2), the Leapfrog scheme (1.3), and the Lax-Wendroff scheme (1.4).

### 1.1 FTCS:

For the FTCS ('Forward in Time and Centered in Space') scheme, we initially set the number of grid points to  $J = 101$ , giving us  $\Delta x = \frac{L}{J-1} = 0.1$ , where  $L$  is the length of the domain of  $x$ . By setting the Courant factor  $C_f$  to 0.5, we obtain  $\Delta t = C_f \cdot \Delta x = 0.05$ . As shown in Figure 1, the initial condition begins to move to the right, as expected. However, the peak of the Gaussian starts to heighten, and soon the entire system is destroyed by perturbations. This behavior occurs because the FTCS method is unstable, meaning that any small perturbation is exponentially amplified over time, as shown by the  $L_2$  norm, ultimately resulting in the total distortion of the initial system.

This instability does not depend on the resolution used, nor on the value of the Courant factor. As shown in the top two plots of Figure 2, increasing the number of points to  $J = 401$  does not prevent  $u(x, t)$  from growing exponentially. In the bottom two panels, we see how the system evolves when we set  $C_f = 0.05$ . Here, we can observe that decreasing  $C_f$  slows down the onset of oscillations, but it does not prevent them. In fact, the FTCS

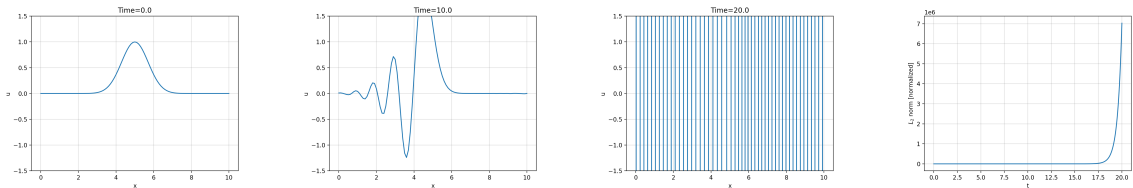


Figure 1: Evolution of the initial system at different times ( $t = 0, 3, 10, 12, 20$ ) evolved using the FTCS scheme. The last plot displays the evolution of the  $L_2$  norm in time.

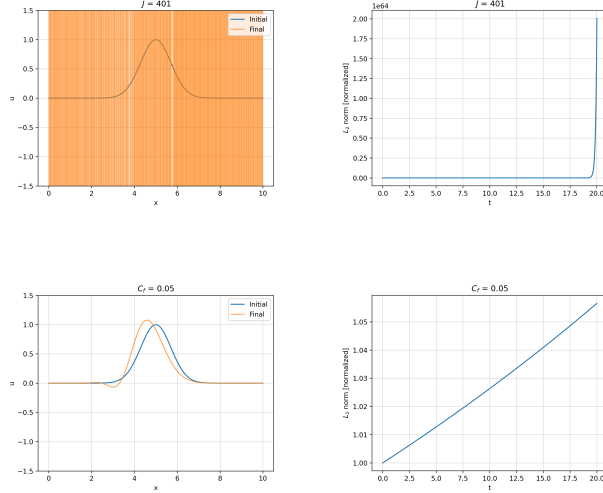


Figure 2: The top two panels shows how the system evolves with an increased resolution. On the bottom two instead, the Courant factor is decreased to  $C_f = 0.05$ .

method is unstable regardless of the value of  $C_f$ , even if the Courant-Friedrichs-Lewy condition ( $C_f \leq 1$ ) is satisfied, as seen in both Figure 1 and Figure 2.

## 1.2 Lax-Friedrichs:

As with the previous method, we begin evolving the system by setting  $J = 101$  and  $C_f = 0.5$ . In Figure 3, we observe that the Lax-Friedrichs method causes the Gaussian to broaden as it travels, due to the presence of a dissipative term in this scheme. Unlike the FTCS method, the Lax-Friedrichs method is conditionally stable; in fact, as long as the CFL condition is satisfied, the  $L_2$  norm decreases over time.

Now, by increasing the number of points to  $J = 501$ , we can see in Figure 4 that the solution at  $t = 20$  is closer to the initial condition than the one obtained with the previous resolution. This is because the dissipative term is proportional to  $\Delta x$ , so as  $J$  increases, the solution experiences less dissipation during its evolution. By changing  $C_f$  to 0.99, we reduce the numerical dissipation further, and the amplitude of the Gaussian at  $t = 20$  becomes very similar to the initial one.

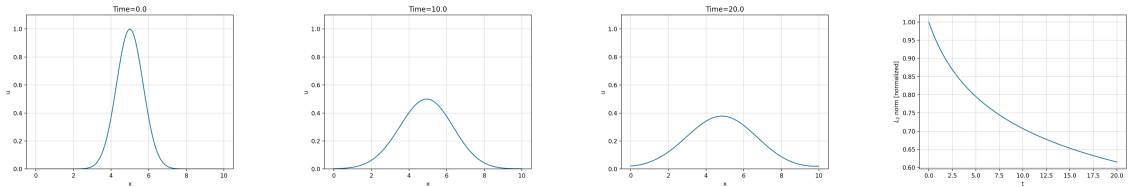


Figure 3: Evolution of the initial system at different times ( $t = 0, 10, 20$ ) evolved using the Lax-Friedrichs scheme. The last plot displays the evolution of the  $L_2$  norm in time.

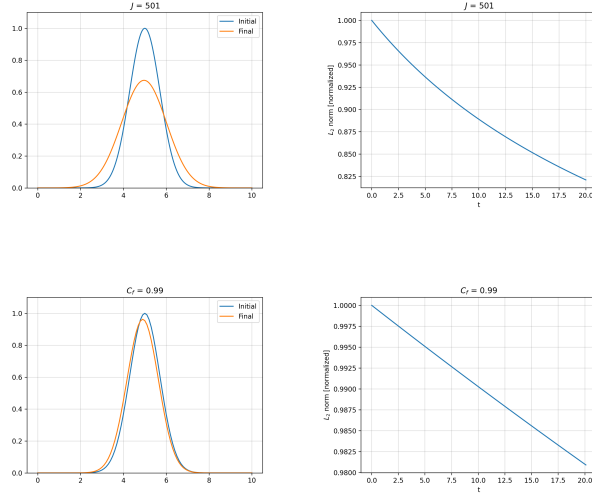


Figure 4: The top two panels shows how the system evolves with an increased resolution. On the bottom two instead, the Courant factor is increased to  $C_f = 0.99$ .

### 1.3 Leapfrog:

As with the previous schemes, we begin by evolving the system using the Leapfrog scheme setting  $J = 101$  and  $C_f = 0.5$ . However, this numerical method requires knowledge of the system's state at two previous time steps, which means that to evolve the system from  $t = 0$  to  $t = \Delta t$ , we would need to know its state at  $t = -\Delta t$ , which we do not. To solve this issue, we perform the first time step using the Lax-Friedrichs method and then continue evolving the system with the Leapfrog method.

In Figure 5, we observe the Gaussian traveling to the right without undergoing significant changes, except for a small perturbation on the left tail of the Gaussian. The  $L_2$  norm shows some oscillations, which are negligible compared to the changes in  $L_2$  seen with the other methods (these oscillations are of the order of  $10^{-5}$  if not normalized).

By increasing the resolution to  $J = 501$ , the numerical solution at  $t = 20$  almost coincides with the initial condition. This significant improvement is due to the Leapfrog scheme being of second order, where the error scales as  $(\Delta x)^2$ . This is not the case for the methods used in Sections 1.1 and 1.2.

Finally, we changed the value of  $C_f$  to 1.5, so that the CFL condition is no longer satisfied. As expected, the solution becomes unstable over time as the  $L_2$  norm grows exponentially.

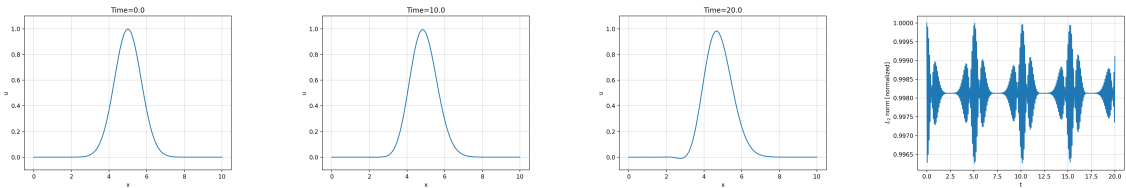


Figure 5: Evolution of the initial system at different times ( $t = 0, 10, 20$ ) evolved using the Leapfrog scheme. The last plot displays the evolution of the  $L_2$  norm in time.

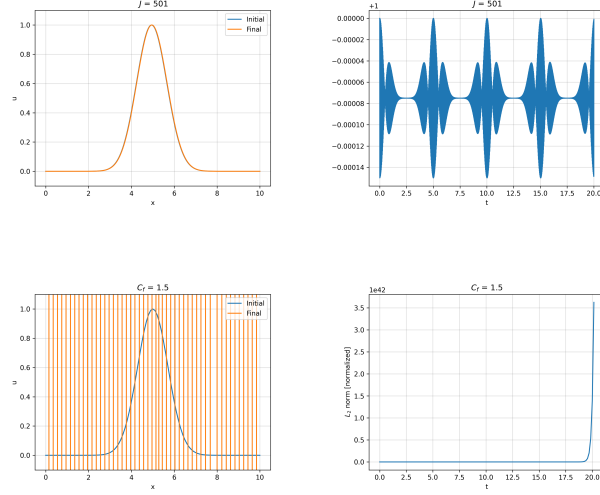


Figure 6: The top two panels shows how the system evolves with an increased resolution. On the bottom two instead, the Courant factor is increased to  $C_f = 1.5$ .

#### 1.4 Lax-Wendroff:

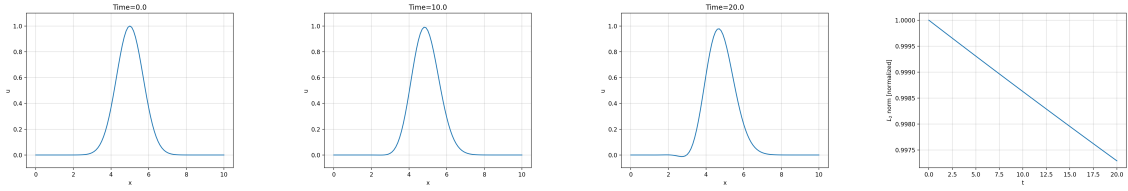


Figure 7: Evolution of the initial system at different times ( $t = 0, 3, 10, 12, 20$ ) evolved using the Lax-Wendroff scheme. The last plot displays the evolution of the  $L_2$  norm in time.

As in the previous sections, we begin by evolving the system using the Lax-Wendroff scheme with  $J = 101$  and  $C_f = 0.5$ . In Figure 1.4, we observe the Gaussian traveling to the right and slightly decreasing in amplitude, while a small oscillation appears on the left tail. These two effects are due to the presence of both dissipative and dispersive terms. Since the CFL condition is satisfied, the  $L_2$  norm does not diverge over time.

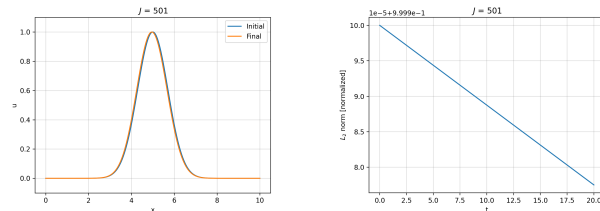


Figure 8: The above panels shows how the system evolves with an increased resolution.

Lastly, we increase the number of points to  $J = 501$ . In Figure 8 we can see how the

dissipative and dispersive terms are now less significant, making the final solution very close to the exact one.

## 2 Step function evolution:

In this section, we will solve the 1D advection equation with an initial condition given by a step function using the Lax-Friedrichs and Lax-Wendroff schemes discussed in Section 1. Considering the domain  $x \in [0, 10]$ , the initial system is defined as  $u(x, t = 0) = 1$  for  $x \in [4, 6]$  and  $u(x, t = 0) = 0$  for the remainder of the domain.

As in the previous sections, we start by setting  $C_f = 0.5$  and  $J = 101$ , and we terminate the evolution at  $t = 20$  using periodic boundary conditions. In Figure 9, we observe that the Lax-Friedrichs scheme introduces both dissipative and dispersive effects (of 2nd and 3rd order, respectively), leading to the appearance of oscillations and a reduction in the overall amplitude of the system.

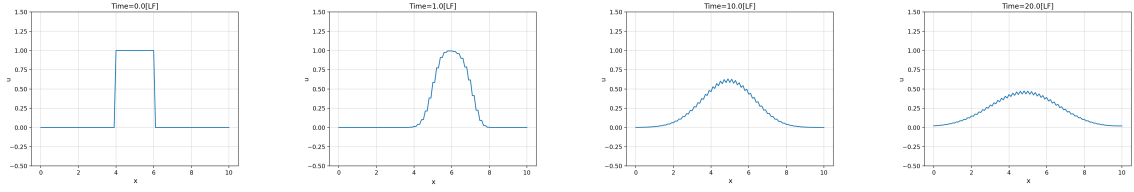


Figure 9: Evolution of the step function at different times evolved using the Lax-Friedrichs scheme.

Figure 10 displays how the step function evolves when using the Lax-Wendroff scheme. Here, we can clearly see the non-monotonicity of this scheme as oscillations are immediately introduced at the edges of the step function.

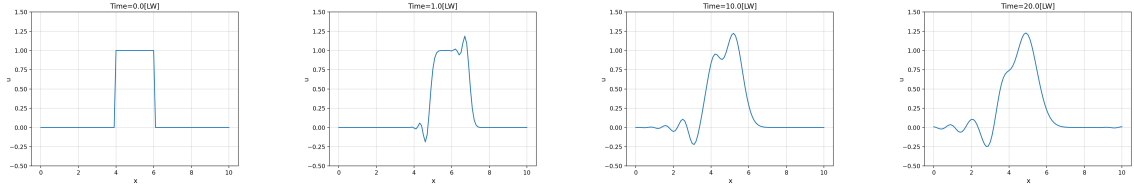


Figure 10: Evolution of the step function at different times evolved using the Lax-Wendroff scheme.

Both methods are conditionally stable; therefore, as  $C_f < 1$ , the  $L_2$  norm does not grow over time, as shown in Figure 11.

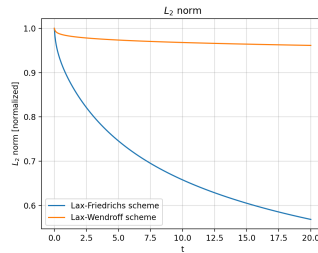


Figure 11: Normalized  $L_2$  evolution in time for both the schemes used to evolve the system. In both cases  $L_2$  decreases as the CFL condition is satisfied.

If we now increase the resolution setting  $J = 401$  for both the schemes used before, we obtain what is shown in Figure 12. If compared to the final solution obtained with less grid points, the ones we now find are less deformed as the dissipative and dispersive terms becomes less significant as  $J$  increases.

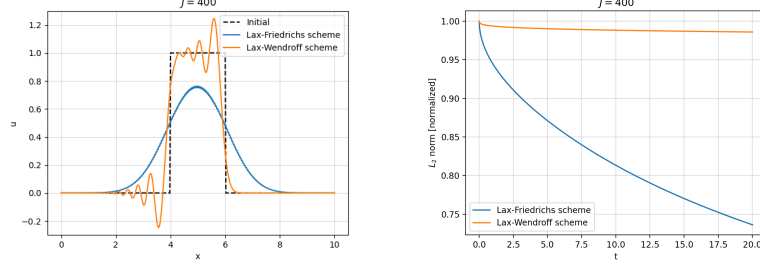


Figure 12: The left panel displays the final state of the system evolved both with the Lax-Friedrichs (in blue) and Lax-Wendroff (in orange) schemes setting  $J = 401$ . On the right panel the time evolution of the  $L_2$  norm is shown.

Finally, if we set  $C_f = 1.1$ , so that the CFL condition is not satisfied anymore, we obtain unstable schemes that introduce major oscillations in the system, as seen in Figure 13.

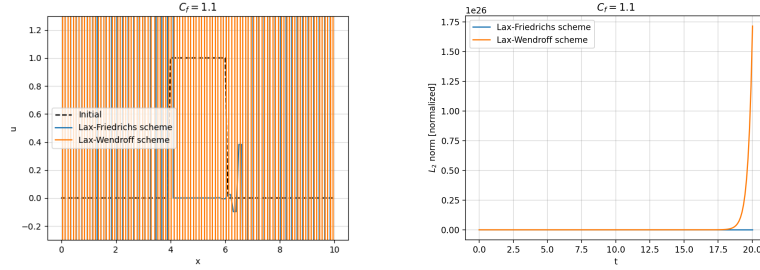


Figure 13: The left panel shows the final state of the initial step function if evolved with both Lax-Friedrichs and Lax-Wendroff schemes having  $C_f > 1$ . On the right panel the time evolution of the  $L_2$  norm is shown.

### 3 Burgers' equation:

In this last section, by using the Upwind scheme, we will evolve a Gaussian according to Burgers' equation both in its Flux-Conservative (FC) and the Non Flux-Conservative (NFC) forms. As done in Section 1, we consider a 1D problem with the domain given by  $x \in [0, 10]$ , with  $u(x, t = 0) = 10 e^{-(x-x_0)^2}$  where  $x_0 = 5$ . We evolve the system up to  $t = 0.5$  applying periodic boundary conditions.

First, we apply the FC form of the Upwind scheme, setting  $C_f = 0.5$  and changing the number of points from  $J = 101$  to  $J = 501$ . As expected, in Figure 14, we can see the formation of a rarefaction wave on the left side and a shock wave on the right side as the Gaussian travels to the right. The position of the shock wave can be computed theoretically, and in this case, it corresponds well with the results obtained through simulations. In particular, by increasing  $J$ , the system at  $t = 0.5$  gets closer to the expected outcome.

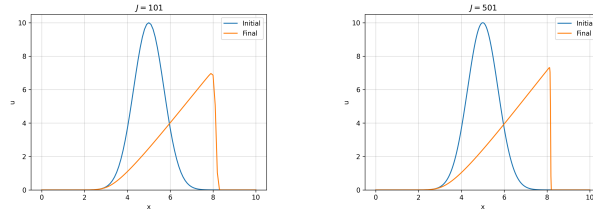


Figure 14: The above panels shows how the system evolves when applying the FC form of the Upwind scheme to solve Burgers' equation. The right panel is obtained setting  $J = 101$ , while the left panel is given by setting  $J = 501$ .

We now evolve the same system, but applying the NFC form of the Upwind scheme. The results, displayed in Figure 15, show how, regardless of the resolution used, such scheme is not capable to converge to the exact solution, as the Hou-Le Flock theorem says. Indeed, the position of the shock wave is not where it is expected to be, despite the fact the the FC and NFC methods are mathematically equivalent.

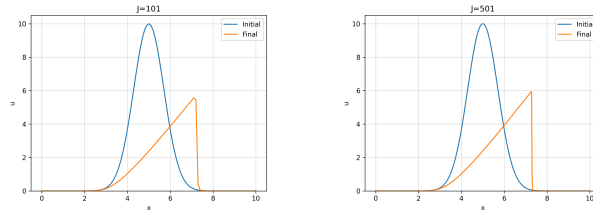


Figure 15: The above panels shows how the system evolves when applying the NFC form of the Upwind scheme to solve Burgers' equation. The right panel is obtained setting  $J = 101$ , while the left panel is given by setting  $J = 501$ .

---

All the codes used to solve the exercises can be found at <https://tinyurl.com/3wfk8694>